The joy of transient chaos

Tamás Tél

Citation: Chaos **25**, 097619 (2015); doi: 10.1063/1.4917287
View online: http://dx.doi.org/10.1063/1.4917287
View Table of Contents: http://scitation.aip.org/content/aip/journal/chaos/25/9?ver=pdfcov
Published by the AIP Publishing

The joy of transient chaos

Tamás Tél
Institute for Theoretical Physics, Eötvös University, and MTA-ELTE Theoretical Physics Research Group, Pázmány P. s. 1/A, Budapest H-1117, Hungary

(Received 10 February 2015; accepted 31 March 2015; published online 28 July 2015)

We intend to show that transient chaos is a very appealing, but still not widely appreciated, subfield of nonlinear dynamics. Besides flashing its basic properties and giving a brief overview of the many applications, a few recent transient-chaos-related subjects are introduced in some detail. These include the dynamics of decision making, dispersion, and sedimentation of volcanic ash, doubly transient chaos of undriven autonomous mechanical systems, and a dynamical systems approach to energy absorption or explosion. © *2015 AIP Publishing LLC*. [http://dx.doi.org/10.1063/1.4917287]

The appearance of chaos with finite lifetime is known as transient chaos (for reviews see Refs. 1 and 2) and provides an example of a "nonequilibrium state" that is different from the asymptotic state, and cannot thus be understood from the asymptotic behavior alone. In such case, one observes a moving around of the system in an apparently chaotic manner and then, often rather suddenly, a settling down to a steady state which is either a periodic or a chaotic motion (but of different type than the transients). Studying only the asymptotic behavior of such dynamics would mean loosing the interesting, chaotic part contained in the transients.

I. INTRODUCTION

My first scientific encounter with transient chaos was at the Dynamics Days conference, held at Twente, Holland, in 1985. For me, one of the highlights was the talk given by Peter Grassberger on their not-yet-published results on systems exhibiting chaos over finite times only. In one of the breaks of the meeting, I came across with his student and coauthor, Holger Kantz, and had a short discussion. I remember, my main question was if the generation of their plots shown in the talk required huge numerical efforts. I had to ask this because, after a postdoc period, I was facing a return to Hungary and could not count there on a particularly strong computational background (in fact, the results of my first papers on transient chaos, e.g., Ref. 3, were obtained using a Commodore 64). In view of the encouraging answer received from Holger, I did not see any reason for not following the attraction I felt towards this phenomenon.

The most appealing features of the talk, and of its published version, the Kantz-Grassberger paper,[4] were that a *nonattracting* set can have consequences observable in practice, and that such sets are of a *very fragile* fractal structure. Nonattracting fractals which are in a mathematical sense sets of measure zero can thus lead in physics to quantities that can be actually measured in experiments!

It became clear for me only afterwards that nonlinear phenomena like crises[5] and basin boundaries[6]—discovered a few years earlier—are also related to such nonattracting chaotic sets. This fact immediately illustrated the broad applicability of transient chaos. Since then, even when my research is not directly related to dynamical systems, I never forget to think of transient chaos if a phenomenon does not find an immediate explanation.

Some of the important morals following from the study of transient chaos can be summarized as follows:

- The traditional view according to which chaos is a long-term, asymptotic property might often be strongly restrictive since it excludes the investigation of transients which might also be of chaotic nature. In fact, in physical terms, asymptotic can only mean that the phenomenon lives on times scales longer than the longest observational time available. Phenomena with lifetimes shorter than this can be just as relevant.
- The resolution of the paradox of physically measuring a nonattracting set of measure zero, mentioned above, is resolved by the fact that following chaos around such a set over long but finite times requires the localization of only a small *neighborhood* of the set (instead of its specification with infinite resolution). This neighborhood is itself of finite volume and, thus, observable.
- Transient chaos plays a similar role in the realm of chaotic systems as an unstable equilibrium point in simple mechanical systems. It is especially well suited to characterize nonequilibrium processes preceding the approach to steady states.
- Transient chaos is an example for a phenomenon where long time single-particle and short time ensemble averages are different. An ensemble of trajectories that stays around the nonattracting chaotic set for a while yields averages characterizing this set, different from the long time asymptotics.
- In invertible systems, we are going to focus on here: the nonattracting set[77] is a *chaotic saddle*. Often, it can be considered to be the union of an infinity of unstable hyperbolic (also called saddle) orbits. A chaotic saddle turns out, however, to be globally less repelling than the component saddle orbits one by one. The fractal structure thus tends to stabilize the saddle dynamically.
- Changing some parameters might lead to an ever weakening repulsion of the saddle. Long term (permanent) chaos arises thus as nothing but a limiting case of transient chaos.

In Sec. II, we summarize some basic properties of transient chaos based on an easily understandable example. In Sec. III, we briefly list typical occurrences of transient chaos in the realm of dynamical systems. Sections IV–VII continue this list with recent examples presented in some detail. Section VIII provides a short summary and outlook.

II. BASIC PROPERTIES OF TRANSIENT CHAOS—AN INTUITIVE VIEW

Transient chaos occurs even in very common every-day-life examples: any system moving irregularly over a period of time and then changing to a regular behavior might be a candidate of transient chaos. For illustrative purposes, we choose such an example, the dispersion of dye (or pollutant material) in a fluid current.

In rivers, in the wake of pillars, piers, or groynes one often observes some kind of accumulation of surface floaters. For very small tracers, the accumulation proves to be temporary, and the particle escapes the wake after some time. Before this happens, it carries out an irregular motion in the wake. The physical background for this is the shedding of vortices from the edges of the obstacle which generates a time-dependent stirring of the fluid within the wake. The lifetime of a tracer within the wake can depend on when and where it enters the wake. Very long lifetimes must be exceptional because the current is tending to transport everything downstream.

A. Geometry and dynamics

It is a real surprise that *nonescaping* tracer orbits, orbits bound to the wake forever, exist, which are of course *unstable*. Their number might even be infinite, nevertheless they do not fill a finite portion of the wake.

Typical tracer trajectories do not hit exactly any of the nonescaping orbits, but might become influenced by the latter. Such tracers follow some of the nonescaping orbits for a while and later turn to follow another one. This wandering among nonescaping orbits results in the chaotic motion of typical tracers over the time span they remain in the wake (downstream of the wake the effect of vortices die out, the flow becomes nearly uniform, and chaotic tracer dynamics is no longer available).

The union of all unstable nonescaping orbits is the *chaotic saddle*. The saddle forms a fractal set with a unique fractal dimension. An example is shown in Fig. 1 where an instantaneous picture of the chaotic saddle is shown in a two-dimensional flow. The fragile nature of this set is reflected by the lack of any line pieces: the chaotic saddle in this representation is a *cloud of points* only (in contrast to chaotic attractors which are filamentary).

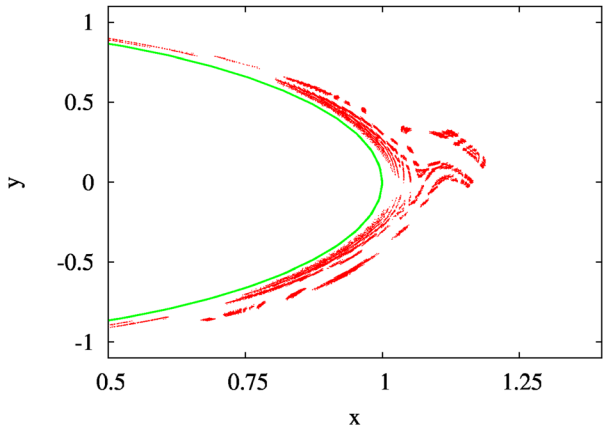

FIG. 1. Instantaneous view of a chaotic saddle (red dots) in the wake of a cylinder of radius unity (green line) in a two-dimensional model of the von Kármán vortex street[7] (flow from left to right) at a Reynolds number where periodic vortex shedding takes place. Tracers started in any red point would never escape the wake neither forward nor backward in time. Note that a stretched horizontal scale is chosen for better visualization. Courtesy of G. Károlyi.

Each nonescaping orbit is of hyperbolic (saddle) type, and therefore the chaotic saddle as a whole also has a stable and an unstable manifold. The *stable manifold* is a set of points along which the chaotic saddle can be reached after an infinitely long time. At a certain instant of time, it can also be considered as the set of initial conditions leading to particle motions that never leave the wake. The stable manifold is thus also of fractal character but this set is filamentary as Fig. 2(a) indicates.

The *unstable manifold* of the chaotic saddle is the set along which particles lying infinitesimally close to the saddle will eventually leave it in the course of time. Its instantaneous form is also a fractal curves, winding in a complicated manner (Fig. 2(b)). When time changes, both the chaotic saddle and its manifolds move.

An appealing feature of the advection problem[8] is that the manifolds (abstract mathematical objects in the theory of dynamical systems) carry clear physical meaning here. For the unstable manifold, this becomes clear by considering a droplet (ensemble) of a large number of tracers which initially overlaps with the stable manifold. As the droplet is advected towards the wake, its shape is strongly deformed,

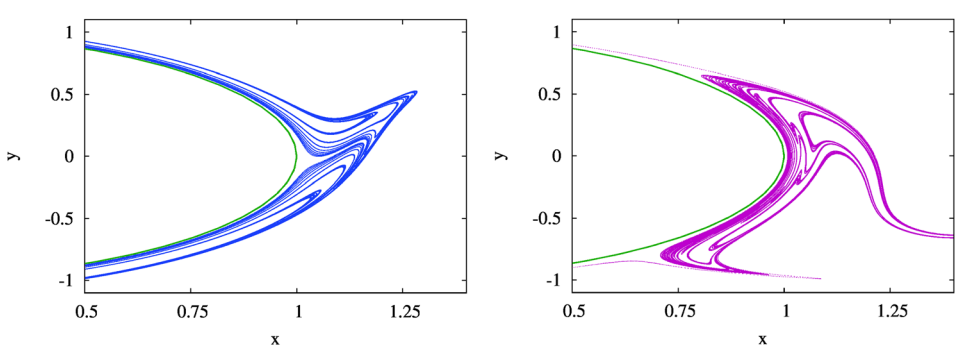

FIG. 2. Stable (left) and unstable (right) manifold of the chaotic saddle in the flow of Fig. 1 at the same instant as there. Both manifolds are fractal curves. The chaotic saddle (the set of red points of Fig. 1) also appears as the intersection of these two manifolds. Courtesy of G. Károlyi.

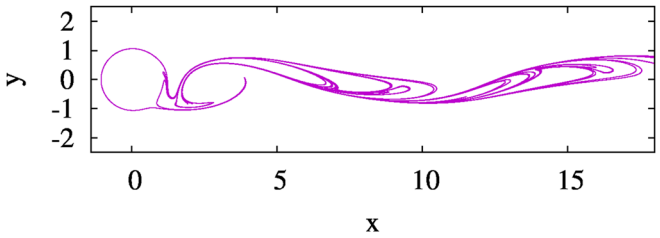

FIG. 3. The fractal unstable manifold of Fig. 2 stretches out of the wake ($0.5 < x < 1.5$) far downstreams. Here, the linear range is much larger and no distortion is applied. Courtesy of G. Károlyi.

but part of the ensemble comes closer and closer to the chaotic saddle as time goes on. Since, however, only a small portion of particles can fall very close to the stable manifold, the majority of the tracers does not hit the saddle and start flowing away from it along the unstable manifold. Therefore, we conclude that in open flows droplets of particles trace out the unstable manifold of the chaotic saddle after a sufficiently long time of observation. The fractal *unstable manifold becomes thus a real physical observable*, something which can be photographed. The unstable manifold stretches out from the wake far downstream, as seen in Fig. 3. Droplet experiments trace out this object indeed.[9,10] It should be kept in mind that far away from the obstacle the fractal pattern is *not* an indicator of chaos in that region; it is rather a fingerprint of transient chaos within the wake transported far downstream by the nearly uniform flow there.

The definition of the chaotic saddle and of its manifolds was given above without any reference to a possible time-periodicity of the flow and of the geometry of the obstacle. In the particular case of time-periodic flows, the chaotic saddle can be decomposed into unstable periodic cycles (similarly as usual chaotic attractors) and the pattern of the saddle and its manifolds repeat themselves with the period of the flow. In the general case of *aperiodic time-dependence*, the only difference is that there are no periodic orbits among the nonescaping ones, and the patterns of the saddle and its manifolds never repeat themselves. If the time-dependence is strong enough and long lasting, these patterns can be seen all the times. (The mathematical background for their proper description is random dynamical systems,[11] and *snapshot* chaotic saddles.[2,12,13]) This is the explanation of the ubiquity of filamentary unstable manifolds visible in experiments[9] and in satellite images showing the oceanic or atmospheric wakes of islands (for an example see Fig. 4). The unstable

FIG. 4. Unstable manifold of a chaotic saddle traced out in a layer of marine stratocumulus clouds in the wake of Guadalupe Island on June 11, 2000, Courtesy of NASA, http://eosweb.larc.nasa.gov/HPDOCS/misr/misr_html/von_karman_vortex.html.

manifold can also be seen as the *main transport route* since tracers escaping the wake after a long time accumulate along this set (see, e.g., Refs. 7, 14, and 15).

B. Characteristic numbers

1. Escape rate

When distributing a large number N_0 of tracers upstream the obstacle, most of them leave the wake eventually. Thus, the probability $p(t)$ of findings points staying still in the wake after time t is a monotonically decreasing function. How rapidly it decreases is an important characteristic of the saddle. The decay is typically exponential

$$p(t) \sim e^{-\kappa t}. \tag{1}$$

The positive number κ is called the escape rate and turns out to be independent of the choice of the initial distribution of the N_0 tarcers. The escape rate is thus a unique property of the chaotic saddle. It measures the saddle's strength of global repulsion. Relation (1) is not necessarily valid from the very beginning, it holds after some time t_0 needed for the ensemble to come sufficiently close to the saddle (t_0 depends thus on the initial condition).[78] As a consequence, this dependence also holds for the average lifetime $\bar{\tau}$ of particles in the wake. As an order of magnitude estimate of $\bar{\tau}$, however, the reciprocal of κ might be a good choice.

2. Topological entropy

The stretching dynamics of typical material lines can be used to define topological entropy. A line segment of initial length L_0 is stretched more and more in the unstable directions. Let $L(t)$ denote the length of the line segment within the wake after time t. After a sufficiently long time this length is known[16] to increase exponentially, and the growth rate is given by just the topological entropy, h, according to the relation

$$L(t) \sim e^{ht}, \tag{2}$$

valid for times longer than some t_0'. The traditional definition based, e.g., on unstable cycles and the one given here are equivalent in time-periodic dynamics. In aperiodic problems, however, only Eq. (2) can be used for the definition of topological entropy. The positivity of h can be considered as a criterion for the existence of (at least) transient chaos. A generalization of the concept of topological entropy, termed expansion entropy, valid in any dimension, just appears in one of the contributions to this focus issue.[17]

3. Natural measure of the saddle, Lyapunov exponents, and dimensions

Just like on a chaotic attractor, there exists a natural probability distribution on any chaotic saddle, too. This is obtained by distributing an ensemble of points around the saddle and following those with long lifetimes. The frequency of visiting different regions of the saddle by these trajectories defines the natural distribution. One can then speak about averages taken with respect to this measure. The largest average Lyapunov exponent $\bar{\lambda}$ on a saddle is positive.

It is worth noting, however, that this is not a unique signal of transient chaos since the Lyapunov exponent is positive even on a single saddle orbit. A unique sign of chaos in such cases (besides $h>0$) is a nontrivial fractality. To this end, the information dimension D_1 of the saddle is a particularly useful tool. The Lyapunov exponent describes the local instability of the saddle, while the escape rate is a global measure of instability. In chaotic cases $\bar{\lambda} > \kappa$,[2] which illustrates that fractality stabilizes the saddle dynamically, as mentioned in the Introduction.

C. Remarks

In the particular example of dispersion in fluid flows, a few further remarks are in order. The precise dynamics of the tracers depends on their size. Very small ones (relative to the size of the obstacle), immediately follow the flow. This implies that in incompressible flows (which are the most typical case) the dynamics is volume preserving, and therefore attracting orbits cannot exists, all tracers must escape the wake. For larger, but still small, sizes Stokes drag is active, and the dynamics is dissipative, attractors might be present. Even if so, they coexist with a chaotic saddle, and have typically small basins of attraction. The shapes of the saddle and its manifolds remain very similar to those of Figs. 1–3.

There is an increasing current interest in *Lagrangian Coherent Structures* (LCSs) of aperiodic flows. They can, loosely speaking, be defined[18,19] as material surfaces shaping the tracer patterns, i.e., as skeletons for the dynamics of tracer ensembles. LCSs exist in all types of aperiodic flows: the elliptic ones are related to extended regions of trapping, and the hyperbolic ones to regions of strong stirring. Among the latter, repelling LCSs separate the fate of initially nearby tracers, while attracting ones identify material surfaces along which particles accumulate after some time. Although these concepts were born outside the realm of transient chaos, it is intuitively clear that in open flows, like flows around obstacles, the repelling (attracting) LCS corresponds to the stable (unstable) manifold of the time-dependent chaotic saddle existing in the wake. What we see in Figs. 3 and 4 can also be considered to be attracting LCSs. The remarkable feature of material accumulation along manifolds made me finish one of my talks, more than a decade ago, with the sentence: "If you are after a good catch, go fishing along an unstable manifold." By now, plankton and larvae on the ocean surface are shown to aggregate from different regions onto such sets, and marine predator birds are found to track LCSs, the analogs of unstable manifolds, in order to locate food patches.[20–22]

III. OCCURRENCES OF TRANSIENT CHAOS

We illustrate with a series of short notes some phenomena from the realm of dynamical systems which find (often surprising) explanations in terms of transient chaos.

A. Periodic windows

Periodic windows are ubiquitous in the chaotic regime of dissipative dynamical systems.[23] In such windows, chaos is present in the sense that there exists an infinity of periodic orbits but their union is not necessarily attractive. Transient chaos thus *always* occurs in such windows both inside the period doubling regime, where the attractor is a cycle of length 2^n with an integer n, and outside these regimes where transient chaos coexists with a small size chaotic attractor: the topological entropy is positive *everywhere* in the window. Since the total measure of windows is known to be finite in the parameter space, just like that of strictly chaotic parameter values, the *probability to find transient chaos is comparable to that of permanent chaos* even in systems known to be chaotic in a traditional sense.

B. Crises

Transient chaos can also be a sign of permanent chaos to be born. More generally, all types of crisis configurations: attractor destructions, explosions, or mergers[5] are accompanied with long lived transient chaos. Large attractors born at crises incorporate into themselves the chaotic saddles existing before. Consequently, the dynamical properties of the saddle are partially inherited by the large attractor. The average time trajectories of the large attractor spend in the region where the saddle existed is practically the same as the reciprocal of the escape rate of transient chaos in the pre-crisis regime. *Transient chaos can thus provide a backbone of the motion on composed chaotic attractors.*

C. Fractal boundaries

Fractal basin boundaries[6] are another common properties of dynamical systems. If two or more simple or chaotic attractors coexist, trajectories may hesitate for a long time before getting captured by one of the attractors. On fractal basin boundaries such trajectories exhibit transient chaos. In fact, *fractal basin boundaries turn out to be stable manifolds of chaotic saddles* existing on the boundary.

D. Controlling chaos

The celebrated Ott-Grebogi-Yorke (OGY) method of controlling chaos[24] is based on the requirement that control sets in if the trajectory visits a preselected target region. The set of points never reaching this target region forms a fractal subset whose escape rate determines the time needed to achieve control. Thus, the OGY method *converts the motion on a chaotic attractor into a kind of transient chaos* before control sets in.

E. Chaotic scattering

For scattering processes in open Hamiltonian problems the *only* way chaos can appear is in the form of transients, because of the asymptotic freedom of the incoming and outgoing motion.[23,25] Trajectories are then trapped in a given region of the configuration space for a while, in which a chaotic saddle also exists. A detailed characterization of the trapping process is based on the so-called delay-time function telling us how the time spent around the chaotic saddle depends on the impact parameters of initial conditions. A unique sign of chaotic scattering is the rather irregular

appearance of the delay-time function. It is *singular exactly in points that lie on the saddle's stable manifold*.

F. Noise induced chaos

In systems subjected to external random forces, the form of the attractor observed might depend on the noise intensity. The phenomenon when a system with simple periodic attractors turns to be chaotic at sufficiently strong (but yet weak) noise is called noise induced chaos.[26,27] In such systems, there is *always* a chaotic saddle coexisting with the simple attractors in the noiseless case. *At increasing noise intensity, the saddle suddenly becomes embedded into a noisy chaotic attractor*, along with the original simple attractors.

G. Transport phenomena

Diffusion and other transport phenomena along a given direction can be interpreted as consequences of chaotic scattering and transient chaos. This deterministic way of describing transport phenomena in a single particle picture is based on the idea of considering an open (scattering) system that is of finite but large extent along a given direction. The phase space is low-dimensional but of large linear size. An analysis of the character of transient chaos leads to the observation that the *escape rate of the saddle can be connected with transport coefficients*.[25,28,29] It is worth mentioning that other characteristics of the chaotic process cannot be expressed solely by means of macro parameters. It is the escape rate alone that has a well defined large-system limit.

H. Complex dynamics preceding thermal equilibrium

Systems approaching thermal equilibrium can possess only fixed point attractors in the space of macroscopic variables. *If a dynamics preceding thermal equilibrium is complex, it must be transiently chaotic*. This is exemplified with stirred chemical reactions in closed containers which are found to exhibit, both theoretically and experimentally,[30,31] long-lasting chaotic transients for sufficiently nonequilibrium initial conditions.

I. Supertransients

Transient chaos also occurs in spatiotemporal dynamical systems having high-dimensional phase spaces. These transients differ from their typical low-dimensional counterparts in that the average lifetime can be extremely long before settling down onto a final attractor which is usually nonchaotic.[5,32] More qualitatively, the escape rate $\kappa(L)$ decreases and tends to zero with the linear size L of the spatially extended system, e.g., exponentially, or as a power of L.[33] In large systems with supertransients, *the observation of the systems' actual attractor is thus very hard*. A notable example is pipe flow turbulence. Around the onset, turbulence is present in the form of localized puffs only, and their lifetime, or the reciprocal of the escape rate, is found to increase superexponentially with the Reynolds number.[34] Puff turbulence is thus a kind of transient chaos.

In Secs. IV–VII, we present a few recent applications of transient chaos, all with some sort of special appeal.

IV. DYNAMICS OF DECISION MAKING

Decision making is strongly related to optimization and is usually formulated in terms of N discrete logical variables x_i, which can be either true or false. The problem is typically subject to a number M of constraints. The goal is to assign truth values to the variables such that all constraints are satisfied. When the fraction M/N is in a critical domain, finding optimal solutions to such constraint-satisfaction problems may be hard. The complexity of problem classes can be measured by the scaling (as function of N) of the time an algorithm needs to find a solution. A hard class of problems is called NP implying that all known algorithms that compute solutions require, in the worst case, exponentially many iterations expressed in terms of the number of variables N.[35] The correctness of a given solution can, however, typically be checked within a polynomial number of iterations. The hardest problems in NP form the subclass of NP-complete problems the solutions to which would enable one to transform any NP problem into this subclass in polynomial time. Applications of these NP-complete cases range from the ground-state problem of Ising spin glasses, via protein folding and Sudoku puzzles, to the travelling salesman problem. According to an interesting recent development of the field, thanks to Ercsey-Ravasz and Toroczkai,[36] constraint-satisfaction problems can be translated into continuous-time *dynamical systems*. As such, they can exhibit chaos. In this exact mapping, each discrete logical variable x_i is replaced by a continuous variable $s_i(t) \in [-1, 1]$, $i = 1, \ldots, N$, where t is a dimensionless time. The range is defined so that $s_i = 1$ (-1) corresponds to the true (false) value. Any constraint is characterized by a function $K_m(\mathbf{s})$, $m = 1, \ldots, M$ (depending on all the s-variables) whose value lies in $[0, 1]$, and K_m vanishes if and only if constraint m is satisfied. The construction of K_m is unique if the constraints are given in a canonical form, the so-called conjunctive normal form.

The dynamics of variables s_i is given as a gradient system

$$\dot{s}_i = -\frac{\partial V(\mathbf{s}, \mathbf{a})}{\partial s_i}, \quad i = 1, \ldots, N, \tag{3}$$

where the potential, or cost, function V is a sum of the squares of the constraint functions weighted with positive factors $a_m(t) > 0$: $V = \sum_{m=1}^{M} a_m(t) {K_m}^2$. Potential V has an absolute minimum at zero for any solution of the problem where all K_m vanish. For large N, function V might have, however, several local minima away from zero. In order to avoid the capturing of the dynamics in any of such minima, Ercsey-Ravasz and Toroczkai chose the weighing factors a_m to be time-dependent according to the dynamics

$$\dot{a}_m = a_m(t) K_m(\mathbf{s}), \quad m = 1, \ldots, M, \tag{4}$$

with some positive initial value, say, $a_m(0) = 1$. Since K_m is nonnegative, the auxiliary variable a_m increases in time (in an approximately exponential manner) as long as the constraint is unsatisfied. If a local minimum due to constraint m is unsatisfied, the exponential growth of a_m guarantees that the local minimum becomes washed out. As a consequence,

for cases with at least one solution, system (3), (4) has the remarkable property that randomly chosen initial conditions $s_i(0)$ lead, with the exception of a set of measure zero, eventually to a solution with $V=0$. Limit cycles do not exist, and the system is shown[36] to *always find* a solution $\mathbf{s}^*$, a fixed point with $|s_i|=1$, of the optimization problem. This property remains true even under noisy perturbations.[37]

If solutions exist, dynamics (3) and (4) can thus exhibit *chaos only in the form of transients*. Furthermore, the difficulty of the solution can be considered to be proportional to the average time needed to find a solution. This opens the way of considering *the escape rate of the transiently chaotic search dynamics to be a measure of the hardness* of the problem instance.

As an example to illustrate the search dynamics, we show a Sudoku puzzle[38] and the characteristic time-dependence of some of the s-variables in Fig. 5. In Sudoku, one has to fill in the cells of a 9×9 grid with integers 1 to 9 such that in all rows, all columns, and in nine 3×3 blocks every digit appears exactly once, while a set of given isolated digits should also be taken into account (see left panel of Fig. 5). These rules and the given digits determine both N and M, the number of independent variables (each empty cell is represented by at most 9 independent logical variables) and constraints, respectively. Sudoku puzzles are designed to have unique solutions. The right panel of Fig. 5 shows the time evolution of the continuous-time dynamics of the 3×3 grid formed by rows 4–6 and columns 7–9. In each cell, there is only one s-variable which converges to 1, the one representing the solution, all the others converge to -1 since they correspond to false digits. The dynamics preceding the asymptotic state is rather complex: all s-values change irregularly, exhibiting long chaotic transients. The solution can be seen to be found in this example after about 150 time units. In other runs even much longer search times are found. In an ensemble of 10^4 randomly chosen initial conditions, the probability that the dynamics has not found the solution by time t follows the rule (1), and the escape rate of the underlying chaotic saddle is obtained to be $\kappa=0.00026$ $(1/\kappa=3850)$.[38]

The authors of Ref. 38 also showed that the escape rate of a puzzle correlates very well with human difficulty ratings. Four categories predefined by the public: easy, medium, hard, and ultra-hard turn out to be related to the escape rate via a logarithmic law. $\eta=-\log_{10}\kappa$ values correspond to them in the ranges $0<\eta\le 1$, $1<\eta\le 2$, $2<\eta\le 3$, and $3<\eta\le 4$, respectively. Puzzles with $\eta>4$ are not known.

A further interesting property of the escape rate of random decision making problems is that in cases when the number N of independent s-variables can change in a broad range, the escape rate is found[36] to decrease as a power of N

$$\kappa(N)=bN^{-\beta}, \tag{5}$$

with an exponent $\beta\approx 5/3$. The transient dynamics of decision making is thus *supertransient*. This law holds for a fixed value of $M/N=4.25$ in the critical region, and illustrates that the escape rate $\kappa(N)$ is a dynamical measure of optimization hardness (thus capable of separately characterising individual instances), while M/N is a static one only. (In the Sudoku problem, which is also high-dimensional, this means that not only the number of the preselected digits is important but also their positioning pattern.)

Equation (5) also implies that the scaling of the average continuous search time $(\approx 1/\kappa)$ is polynomial. Nonetheless, the exponential scaling characteristic to NP-complete problems does not disappear, but appears when measuring the number of *integration steps* needed (using adaptive Runge-Kutta methods).

V. VOLCANIC ASH DISPERSION

The volcanic eruption of Eyjafjallajökull on Iceland in 2010 lead to concerns that volcanic ash would damage aircraft engines, and the controlled airspace of many European countries was closed resulting in the largest air-traffic shutdown since World War II. The closures caused millions of passengers to be stranded not only in Europe, but across the world. Not much later, the Fukushima accident (2011) lead to increased public concern regarding pollutant spreading from industrial accidents. These recent events underlined the need for investigating pollutant dispersion in the atmosphere. Aerosol particles from different sources may be advected far away from their initial position and may cause air pollution episodes at distant locations.

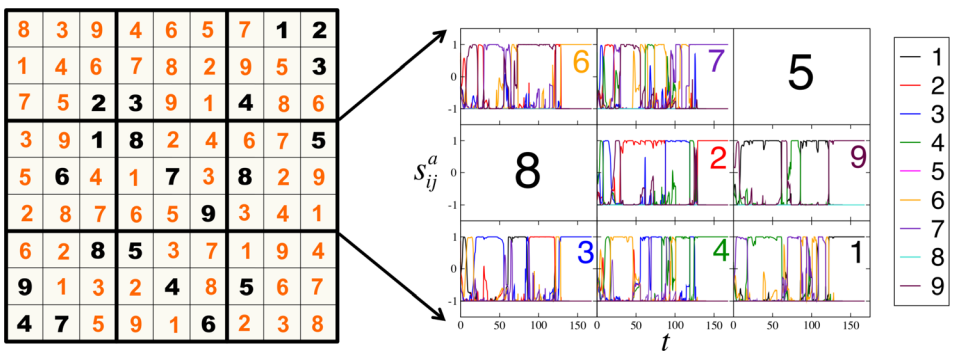

FIG. 5. Transient chaos preceding the finding of the Sudoku solution in the search dynamics (3), (4). The puzzle given in the left panel is one of the hardest: with the 21 given digits, it corresponds to $N=257$, $M=2085$. The time-dependence of the variables s_{ij}^a (representing digit a, colored as in the color bar on the right) in cell i, j is shown in the right panel. In each cell there are 9 running trajectories but many of them are on top of each other close to -1. Courtesy of M. Ercsey-Ravasz and Z. Toroczkai.

Current numerical capacity enables us to monitor *individual* aerosol particles one by one. These trajectories turn out to be chaotic, and an ensemble of trajectories can be used to predict statistical properties, e.g., the average deposition dynamics.

In order to track individual aerosol particles with realistic size and density, the equation of motion for the particle trajectory $\mathbf{r}(t)$ is derived from Newton's equation. Scale analysis reveals that the horizontal velocity of a small aerosol particle takes over the actual local wind speed practically instantaneously, whereas vertically the terminal velocity w should be added to the vertical velocity component of air.[39,40] w depends on the radius r and density ρ_p of the particle, as well as, on the density ρ and viscosity ν of the air at the location of the particle

$$\dot{\mathbf{r}} = \mathbf{v}(\mathbf{r}(t), t) + w\mathbf{n}, \tag{6}$$

where $\mathbf{v}(\mathbf{r}, t)$ is the wind field at point $\mathbf{r}$ and time t, and $\mathbf{n}$ is the vertical unit vector pointing downwards. Realistic aerosol particles not falling out within hours are of radius of at most 12 μm, and have a density of about $\rho_p = 2000$ kg/m^3. For them, Stokes' law is valid during the full motion, and hence the terminal velocity is $w = 2\rho_p r^2/(9\rho\nu g)$. As an input to dispersion simulations, the reanalysis data of *measured* wind fields can be used, which are accessible, e.g., in the ERA-Interim database.[41] The wind velocity at the actual location of a particle is calculated using spline interpolations in both space and time.

Mount Merapi in Indonesia had long-lasting eruption series in 2010, from late October to November. As an example of the outfall dynamics of aerosol particles, instead of a continuous eruption, we consider a single imagined volcanic ash puff. It has an initially columnar shape of size $1^\circ \times 1^\circ \times 400$ hPa (in the vertical, pressure coordinates are used), containing $n_0 = 2.16 \times 10^5$ particles of radius $r = 5\,\mu$m centered at Mount Merapi at the height of about 5 km ($p_0 = 500$ hPa), and is emitted at 00 UTC on 1 November 2010.[39] The particles spread and reach very different regions in the atmosphere since, entering into different vertical levels, they become subject to different horizontal winds. 20 days after the hypothetical emission, the particles cover a huge area and are well mixed in the midlatitudes of the Southern Hemisphere.

One measurable consequence of the aerosol dynamics (6) is the outfall. The upper panel of Fig. 6 shows in brown the location of all the deposited particles in the period 1–20 November 2010. There are large regions without any outfall, and the overall pattern is filamentary.

A careful study of the particle dynamics leads to the conclusion that long lived aerosol particles come close, much before deposition, to a *global atmospheric chaotic saddle*. The escape rate is found in our example to be $\kappa = 0.103$ day^{-1} (in harmony with an average lifetime of about 10 days). The existence of transient chaos is also supported by the fact that topological entropies, as defined by (2), are measured to be positive, on the order of 0.5 day^{-1}.[42] This atmospheric saddle is an example for a case of aperiodic time-dependence.

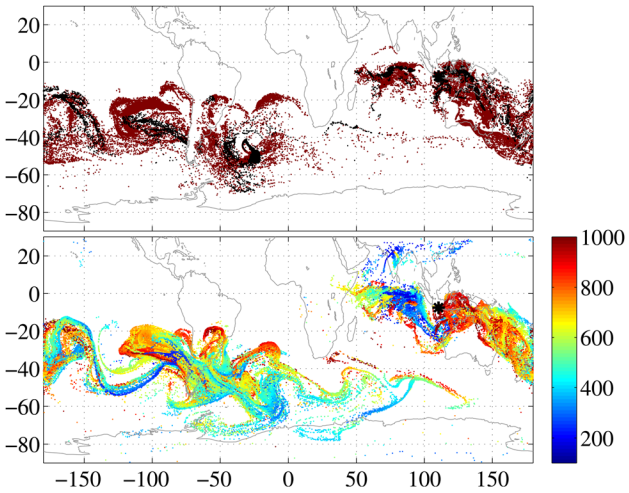

FIG. 6. Dispersion of volcanic ash consisting of $r = 5\,\mu$m particles of density $\rho_p = 2000$ kg/m^3 from the eruption of Mount Merapi (110.44° E, 7.54° S, black asterisk) described in the text. The upper panel shows the outfall integrated up to the 20th of November (brown dots). Black dots represent the outfall during November 18. The lower panel illustrates the spatial distribution of the aerosol particles still in the air at 12 UTC on 18 November 2010. Colorbar indicates the pressure level of the particles in hPa. It is worth noting the high latitude of many particles (blueish colors) and that there is hardly any material exchange between the two hemispheres over the time scale of a few weeks. Courtesy of T. Haszpra.

The dynamical systems' view enables us to give a novel interpretation of the outfall. The set of deposited particles on the surface can be specified, in the language of transient chaos theory, as the *intersection of the unstable manifold of the global atmospheric chaotic saddle with the surface*. Considering a shorter period, a single day (black dots in Fig. 6, upper panel), the filamentary nature of the outfall pattern is more pronounced (an exact fractal is expected for an instantaneous outfall pattern only). The lower panel of Fig. 6 indicates the location of the not yet deposited particles in a given time instant: at noontime of the 18th day after the eruption (12 UTC on 18 November 2010). Since the majority of these particles are on their way towards the surface, they practically trace out the *unstable manifold of the saddle*. This figure thus corresponds to Fig. 3 but in a three-dimensional setting, the coloring indicating the height, more precisely the pressure level of the particles.[79]

It is remarkable that the escape rate as a function of the particle radius r is found to range over about two orders of magnitude although the radii vary over one decade only. The dependence is thus strongly nonlinear. The best approximate fit up to $r = 12\,\mu$m appears to be exponential[39]

$$\kappa(r) \sim \exp(kr), \tag{7}$$

with $k \approx 0.46\ \mu\text{m}^{-1}$, a very strong parameter-dependence in this low-dimensional, but spatially extended dynamical problem.

VI. DOUBLY TRANSIENT CHAOS

After the appearance of our introductory textbook,[43] Adilson Motter came to me and asked why we had claimed that the dynamics of magnetic pendula was chaotic. My naive answer was a hint on the easily observable irregular

motion of the pendulum before settling down at some of the magnets, and on the obvious fractality of the basin boundary displayed in many publications (for example, see Fig. 7). But the point was well taken, in such dissipative systems without any driving all motion must eventually cease because of the monotonous decay of the energy. We decided to carry out a systematic investigation of the problem which leads to the conclusion that transient chaos as presented in Sec. II is only one option, another class, termed doubly transient chaos,[44] also exists within which the dynamics is even more fragile than in usual transient chaos.

A detailed investigation reveals that two trajectories in different basins tend to separate from each other over a relatively short period of time but they do so exponentially fast, they thus possess positive finite-time Lyapunov exponents. Fast separation takes place when the speed of the pendulum is low, as it would be expected when an orbit approaches an unstable fixed point embedded in usual chaotic saddles. The dynamics, however, does not have any periodic cycle, long-term instability can only be due to a few fixed points (of saddle type). One observes, nevertheless, that during the period of rapid separation the trajectories wander erratically in the vicinity of a set that plays the role of a chaotic saddle. This set can be estimated from the positions where the trajectories separate exponentially from each other. However, this set consists of only *pieces of trajectories* in the phase space and—in contrast to usual saddles, e.g., the one shown in Fig. 1—is not an invariant set of orbits. Moreover, this set manifests itself only during the period of exponential separation, which motivates us to refer to it as a *transient chaotic saddle*.

This view is supported by the observation of the individual lifetimes spent far away from any attractor obtained for trajectories which started on a straight line with zero initial velocity. This function is highly irregular, and appears to exhibit a few isolated infinitely high peaks only (in contrast to traditional systems where infinities sit on a fractal set). In our case, subsequent magnifications indicate that the set of long lifetimes becomes increasingly sparse at sufficiently small scales.

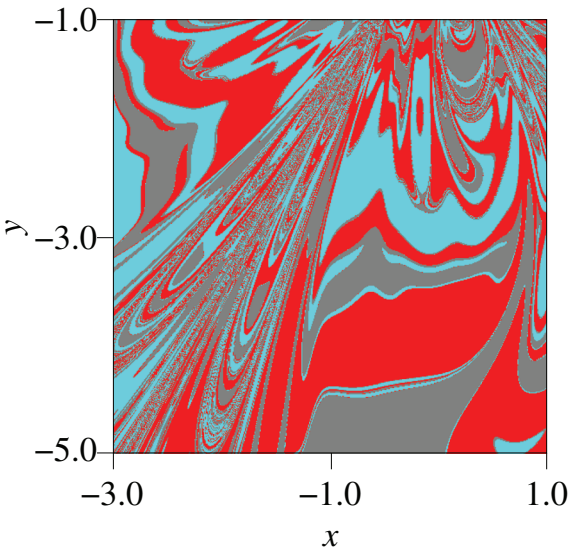

FIG. 7. Part of the basin structure of a magnetic pendulum with three magnets at the corner of a regular horizontal triangle of unit edge length around the origin. A part of the plane of initial positions is shown, where points with vanishing initial velocity are colored according to the magnet in which neighborhood the pendulum settles down. Most observers would consider this pattern to be fractal. Courtesy of G. Károlyi.

This leads us to the conclusion that perhaps a *time-dependent escape rate* would provide a proper characterization of the dynamics. We define[44] this as the instantaneous rate $\kappa(t)$ of decay of the fraction $p(t)$ of still unsettled trajectories at time t

$$\dot{p}(t) = -\kappa(t)p(t). \tag{8}$$

Numerical results indicate that $\kappa(t)$ is an exponentially increasing function in this example. The survival probability thus decays superexponentially, i.e., the escape dynamics speeds up as times goes on.

In harmony with the time-dependence of the escape rate, we find that the fractality of the basin boundary is *scale-dependent*. Considering smaller and smaller scales, the fractal dimension of the set separating the different colors is found to decrease and tend to unity.[44] This can indeed be seen when considering subsequent magnifications of Fig. 7 as illustrated by Fig. 8.

It is interesting to observe that the character of chaos immediately changes when driving is added. By moving the plate of the magnets up and down in a sinusoidal manner, unstable periodic orbits immediately appear, and the long term dynamics is governed by a usual chaotic saddle (in coexistence with periodic attractors). For small driving amplitudes, the time-dependent escape rate (8) initially increases, but then levels off at a finite constant value, and the crossover period shrinks with the amplitude.

In summary, our principal results are that in undriven systems: (i) the measured dimension of the basin boundaries can be noninteger and the finite-time Lyapunov exponents can be positive over finite scales but neither holds true asymptotically; (ii) the basin boundaries have (asymptotic) integer fractal dimensions; (iii) the survival probability outside the attractors changes dramatically, characterized by a time-dependent escape rate; (iv) transient behavior is governed by a transient chaotic saddle that is prominent over a specific energy interval. This doubly transient chaos appears to be *the generic form of chaos in autonomous (nondriven)*

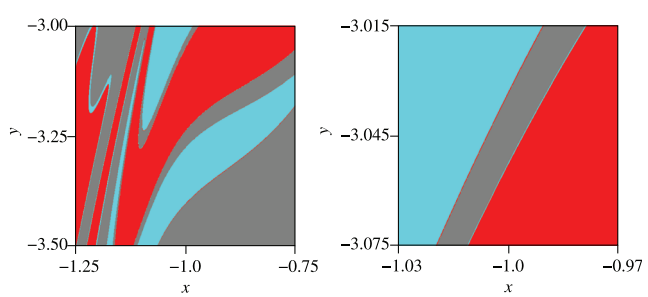

FIG. 8. Blowing up the basin structure. Left panel: magnification of a small square from the most fractal-looking lower left quadrant of Fig. 7. Right panel: magnification of a small square of the left panel. The dilution of fractality can be seen by naked eye. Courtesy of G. Károlyi.

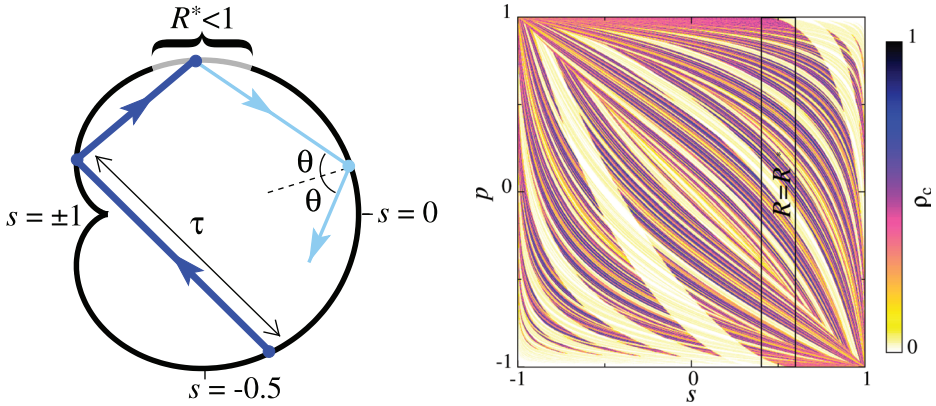

FIG. 9. Energy escape in a two-dimensional billiard. Left panel: billiard with partial reflectivity, the width of the ray is proportional to its intensity (J). The reflection coefficient $R = R^* = 0.1$ in the gray boundary interval, at other locations there is no absorption: $R = 1$. Right panel: c-density with color coding. The corresponding escape rate is $\kappa = 0.058$. Birkhoff coordinates $\vec{x} = (s, p = \sin\theta)$ are used, where s is the arc length along the boundary and θ is the collision angle. Courtesy of E. G. Altmann and J. S. E. Portela.

dissipative systems, with the double pendulum and many every-day phenomena as examples.

VII. DYNAMICAL SYSTEMS WITH ABSORPTION/ EXPLOSION

Certain physical problems related to wave dynamics in the short wavelength limit can be represented by particles moving along simple trajectories but carrying with them certain physical quantities which change in time according to some rule. One example is the decay of sound intensity in hall acoustics, which can be understood by considering sound rays (particles) bouncing with constant velocity within a billiard (the hall) which loose a portion of a quantity (the energy) carried with them upon each collision with the wall. This loss of energy corresponds to sound attenuation or absorption in general. In such systems, it is *not the particles (matter) what escapes rather the energy content*, a quantity carried along with the particles.

The usual dynamical systems' approach should somewhat be broadened for a proper description of such problems. Consider a discrete-time representation $\vec{x}_{n+1} = f(\vec{x}_n)$, a proper Poincaré map of a time-continuous flow. One can fully reconstruct the continuous-time dynamics if the return time distribution $\tau(\vec{x})$ [chosen as the time between $\vec{x}$ and $\vec{x}' \equiv f(\vec{x})$] is known and the sum of return times is followed along the map trajectory.[25] The novel feature is that besides the return time, the evolution of an intensity-like quantity J should also be monitored. This quantity can be represented to change only upon intersections with the Poincaré surface, when its value becomes suddenly smaller. The amount of this change is specified by the distribution $R(\vec{x})$ of reflection coefficients, a quantity assumed to be known on the Poincaré surface (just like $\tau(\vec{x})$). Instead of the usual map f, one then follows an extended map f_{ext} which implies extending the map's phase space $\vec{x}_n$ by two further variables t_n and J_n: the time at intersection n with the surface, and the intensity just before this intersection.[45] The extended map thus reads as

$$f_{\text{ext}} : \begin{cases} \vec{x}_{n+1} = f(\vec{x}_n), \\ t_{n+1} = t_n + \tau(\vec{x}_n), \\ J_{n+1} = J_n R(\vec{x}_n). \end{cases} \tag{9}$$

Instead of individual trajectories in the extended phase space, it is worth studying here also an ensemble of trajectories, and their energy density $\rho(\vec{x}, t)$. In analogy with the problem of room acoustics, we consider closed chaotic maps $f(\vec{x}_n)$ and find[45] that for any smooth initial intensity distribution $\rho(\vec{x}, t = 0)$ there is an overall exponential decay, multiplied by a distribution $\rho_c(\vec{x})$ depending only on the spatial coordinates so that for long times

$$\rho(\vec{x}, t) \sim e^{-\kappa t} \rho_c(\vec{x}). \tag{10}$$

Exponent $\kappa > 0$ is called again the escape rate but, remember, it is a measure of the *energy escape* since there is no particle escape as map f is assumed to be closed.[80] Both κ and ρ_c are found to be independent of initial conditions. Writing (10) as $\rho_c(\vec{x}) \sim e^{\kappa t} \rho(\vec{x}, t)$ shows that ρ_c is kind of a limit distribution obtained by *compensating* for the energy loss by homogeneously injecting energy exactly at the rate of κ. Density ρ_c is therefore called the conditionally invariant

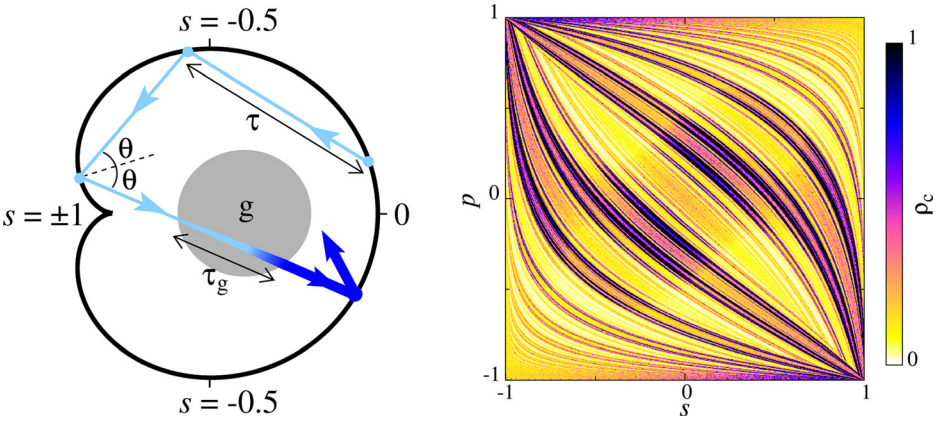

FIG. 10. Energy explosion in the same billiard as in Fig. 9. Left panel: billiard with a gain region in the middle (gray disc, marked by g), the width of the ray is proportional to its intensity (J). The reflection coefficient upon collision with the wall is $R = e^{\tau_g} \geq 1$, where τ_g is the time the trajectory spends in the gain region. Right panel: c-density with color coding. The corresponding explosion rate is $-\kappa = 0.215$. Courtesy of E. G. Altmann and J. S. E. Portela.

density (c-measure) in analogy with a quantity introduced as the density of points conditioned to escape after a long stay only in usual open systems with transient chaos.[46] c-density ρ_c can be normalized to unity over the phase space of map f. The c-density is found to be a complicated fractal measure with a nontrivial information dimension, as illustrated by Fig. 9. The filamentary pattern suggests that this density is concentrated on the unstable manifold of the intensity dynamics (as in usual transient chaos), and one can also find the underlying chaotic saddle in the extended map.

Within this extended set-up one can even find a physical interpretation for *negative escape rates*. Optical microcavities provide a representative example of such systems. Lasing modes are induced by the gain medium present in the cavities and only long-living light rays are able to profit from this gain. For strong enough gain, when the reflection coefficient is larger than unity: $R(\vec{x}) > 1$, in certain regions at least, the overall intensity $\rho(\vec{x}, t)$ *increases in time*, in an exponential fashion.[47] Equation (10) remains thus valid, just with a negative κ. Quantity $-\kappa$ can be called the *explosion rate*. It is perhaps a surprise that the c-density does not lose its fractal measure property as Fig. 10 demonstrates.

It is instructive to see that there exists a *unified framework* valid both for absorbing and exploding cases that also shows how κ and the c-density are related. For invertible f-dynamics, this can be written as a discrete-time Perron-Frobenius-type equation[45,47] (see also Ref. 48) acting on the density function ρ_n of the extended map at discrete time n as

$$\rho_{n+1}(\vec{x}') = e^{\kappa\tau(\vec{x})}\frac{R(\vec{x})\rho_n(\vec{x})}{|\mathcal{D}_f(\vec{x})|}. \tag{11}$$

Here, $\mathcal{D}_f(\vec{x})$ is the Jacobian of the Poincaré map f at the phase space coordinate $\vec{x}$ (in the billiard examples, of course, $\mathcal{D}_f(\vec{x}) = 1$). Iteration scheme (11) expresses, in a more advanced form, the compensation mechanism mentioned above in relation to (10): when compensating escape (explosion) by injecting (extracting) energy via a multiplication with $e^{\kappa\tau(\vec{x})}$ per iteration, a time-independent limit-distribution $\rho_\infty(\vec{x})$ is reached. This only happens if κ is the valid escape rate, and then the limit distribution is the corresponding c-density: $\rho_\infty(\vec{x}) = \rho_c(\vec{x})$. Integrating (11) over $\vec{x}'$ with the c-density on both sides, and using the normalization of ρ_c, one finds

$$\langle e^{\kappa\tau}R\rangle_c = 1, \tag{12}$$

where the average is taken with respect to the c-measure. This expresses an intimate relation: κ and ρ_c are selfconsistently adjusted so that the average of the compensated reflection coefficient $e^{\kappa\tau}R$ should be unity (a sign of stationarity) when the average is taken just with the c-measure. Quantities κ and ρ_c can also be considered as the parameter making the eigenvalue of the operator defined by (11) to be unity and the eigenfunction belonging to this largest eigenvalue, respectively. It is immediate from (12) that for $R > 1$, in sufficiently extended regions at least (i.e., the case of explosion), κ must be negative.

One can also find[45,47] a general relation between the fractality of ρ_c, the distributions $\tau(\vec{x}), R(\vec{x})$, and properties of the extended map. The information dimension $D_1^{(1)}$ of the chaotic saddle along the unstable foliation of two-dimensional extended maps can be expressed as

$$D_1^{(1)} = 1 - \frac{\kappa\bar{\tau} + \overline{\ln R}}{\bar{\lambda}}, \tag{13}$$

where the averages denoted by overbars are taken over the *chaotic saddle* of this map. It is remarkable that the dimension can be expressed in such a simple way. Besides the escape rate κ and the positive average Lyapunov exponent $\bar{\lambda}$ only the averages $\bar{\tau}$ of the return times and $\overline{\ln R}$ of the logarithm of the reflection coefficients appear.[81] This result is an extension of the Kantz-Grassberger formula $D_1^{(1)} = 1 - \kappa/\bar{\lambda}$, valid for the partial dimension in usual transient chaos. The beauty of this generic and simple relation connecting fragile (since $D_1^{(1)} < 1$) fractality and dynamics, which I first saw during that 1985 Dynamics Days, certainly contributed to my continuous attraction towards transient chaos.

VIII. OUTLOOK

I would like to end with a brief summary of further transient-chaos related subjects, which might be at least as interesting as the ones just presented in some detail above. *Leaky dynamical systems* arise when artificial holes are introduced into closed dynamics, and the study of the resulting transient dynamics reveals relevant features of the closed dynamics, including Poincaré recurrences.[48] *Almost invariant sets* are subsets of larger systems points of which remain bound to this subset for a long time. They are thus natural candidates for characterizing Lagrangian coherent structures,[19] and other environment-related phenomena.[49] Transient chaos theory can also be used to understand the origin of transients and *extreme events* in excitable systems,[50,51] long spatio-temporal transients in *chimera states*,[52,53] *memory effects* in particle dispersion in open flows,[54] and to gain a deeper insight into the *nature of turbulence*.[55] Recent developments in classical chaotic scattering include the investigation of the ray dynamics in optical *metamaterials*,[56] of escape in celestial mechanics[57,58] and in medically relevant fluid flows,[59,60] and a basic understanding of the structure of chaotic saddles underlying scattering in *higher dimensions*.[61–64]

Snapshot chaotic saddles and attractors exist in aperiodically driven system,[65] and represent instantaneous states of ensembles of trajectories. A novel observation of recent years is that they are uniquely defined not only in noisy systems[66] but also in the presence of smooth driving that might even be a one-sided temporal shift of some parameters. This property makes the concept very well suited for an application in climate dynamics.[67–69] The observed robust existence of chaotic snapshot attractors over a wide range is a consequence of the presence of transient chaos in the undriven system: the dynamics on snapshot attractors might thus be considered driving-induced-chaos (in analogy with noise-induced-chaos).

Quantum aspects cannot be left without a very short mention. Features related to open channels in quantum systems appear in properties such as the fractal distribution of

eigenstates,[70] the fractal Weyl's law,[71,72] and quantum transport,[73] including transport in graphene.[74] The investigation of these quantum properties is also subject of active recent research (see, e.g., Refs. 48, 75, and 76).

My final conclusion can only be: *Keep an eye on the potential appearance of transient chaos since this phenomenon is an inexhaustible source of challenge and inspiration.*

ACKNOWLEDGMENTS

This work was supported by OTKA Grant No. NK100296. The support of the Alexander von Humboldt Foundation is acknowledged. Special thank is due to E. Altmann, M. Ercsey-Ravasz, T. Haszpra, G. Károlyi, J. S. Portela, and Z. Toroczkai who helped with preparation of figures for this paper. Insightful discussions with them and with T. Bódai, A. Daitche, G. Drótos, U. Feudel, M. Ghil, K. Guseva, G. Haller, C. Jung, T. Kovács, Y.-C. Lai, A. Motter, and M. Vincze are deeply acknowledged.

[1]T. Tél, in *Directions in Chaos*, edited by B.-l. Hao (World Scientific, Singapore, 1990), Vol. 3, pp. 149–221; T. Tél, in *STATPHYS 19: The Proceedings of the 19th IUPAP Conference on Statistical Physics* (World Scientific, Singapore, 1996), pp. 346–362.
[2]Y.-C. Lai and T. Tél, *Transient Chaos, Complex Dynamics on Finite-Time Scales* (Springer, New York, 2011).
[3]T. Tél, Phys. Rev. A **36**, 1502 (1987).
[4]H. Kantz and P. Grassberger, Physica D **17**, 75 (1985).
[5]C. Grebogi, E. Ott, and J. Yorke, Phys. Rev. Lett. **48**, 1507 (1982); Physica D **7**, 181 (1983).
[6]C. Grebogi, E. Ott, and J. Yorke, Phys. Rev. Lett. **50**, 935 (1983).
[7]C. Jung, T. Tél, and E. Ziemniak, Chaos **3**, 555 (1993).
[8]H. Aref, J. Fluid Mech. **143**, 1 (1984).
[9]J. C. Sommerer, H. Ku, and H. Gilreath, Phys. Rev. Lett **77**, 5055 (1996).
[10]M. Van Dyke, *An Album of Fluid Motion* (Parabolic Press, Stanford, 1988).
[11]F. Ladrappier and L.-S. Young, Commun. Math. Phys. **117**, 529 (1988).
[12]J. Jacobs, E. Ott, T. Antonsen, and J. Yorke, Physica D **110**, 1 (1997).
[13]Z. Neufeld and T. Tél, Phys. Rev. E **57**, 2832 (1998).
[14]I. Scheuring, T. Czárán, P. Szabó, G. Károlyi, and Z. Toroczkai, Origins Life Evol. Biosphere **33**, 319 (2002).
[15]Z. Neufeld and E. Hernández-Garcia, *Chemical and Biological Processes in Fluid Flows* (Imperial College Press, London, 2010).
[16]S. E. Newhouse and T. Pignataro, J. Stat. Phys. **72**, 1331 (1993).
[17]B. R. Hunt and E. Ott, Chaos **25**, 097618 (2015).
[18]G. Haller and G. Yuan, Physica D **147**, 352 (2000).
[19]G. Haller, Annu. Rev. Fluid Mech. **47**, 137 (2015).
[20]M. Sandulescu, C. E. López, E. Hernández-Garcia, and U. Feudel, Ecol. Complexity **5**, 228 (2008).
[21]C. S. Harrison, D. A. Siegel, and S. Mitarai, Mar. Ecol. Prog. Ser. **472**, 27 (2013).
[22]E. T. Kai *et al.*, Proc. Natl. Acad. Sci. **106**, 8245 (2009).
[23]E. Ott, *Chaos in Dynamical Systems*, 1st ed. (Cambridge University Press, Cambridge, 1993); *Chaos in Dynamical Systems*, 2nd ed. (Cambridge University Press, Cambridge, 2002).
[24]E. Ott, C. Grebogi, and J. Yorke, Phys. Rev. Lett. **64**, 1196 (1990).
[25]P. Gaspard, *Chaos, Scattering and Statistical Mechanics* (Cambridge University Press, Cambridge, 1998).
[26]M. Iansity, Q. Hu, R. M. Westervelt, and M. Tinkham, Phys. Rev. Lett. **55**, 746 (1985).
[27]Y.-C. Lai, Z. Liu, L. Billings, and I. B. Schwartz, Phys. Rev. E **67**, 026210 (2003).
[28]J. Vollmer, Phys. Rep. **372**, 131 (2002).
[29]R. Klages, *Macroscopic Chaos, Fractals and Transport in Nonequilibrium Statistical Mechanics* (World Scientific, Singapore, 2007).
[30]S. Scott, B. Peng, A. Tomlin, and K. Showalter, J. Chem. Phys. **94**, 1134 (1991).
[31]J. Wang, P. G. Sorensen, and F. Hynne, J. Phys. Chem. **98**, 725 (1994).
[32]Y.-H. Do and Y.-C. Lai, Phys. Rev. Lett. **91**, 224101 (2003).
[33]J. P. Crutchfield and K. Kaneko, Phys. Rev. Lett. **60**, 2715 (1988).
[34]B. Hof, A. de Lozar, D. J. Kuik, and J. Westerweel, Phys. Rev. Lett. **101**, 214501 (2008).
[35]M. R. Garey and D. S. Johnson, *Computers and Intractability: A Guide to the Theory of NP-Completeness* (W. H. Freeman, New York, 1990).
[36]M. Ercsey-Ravasz and Z. Toroczkai, Nat. Phys. **7**, 966 (2011).
[37]R. Sumi, B. Molnár, and M. Ercsey-Ravasz, Eur. Phys. Lett. **106**, 40002 (2014).
[38]M. Ercsey-Ravasz and Z. Toroczkai, Sci. Rep. **2**, 725 (2012).
[39]T. Haszpra and T. Tél, Nonlinear Processes Geophys. **20**, 867 (2013).
[40]T. Haszpra and A. Horányi, Idojaras: Q. J. Hung. Met. Serv. **118**, 335 (2014).
[41]D. P. Dee *et al.*, Q. J. R. Meteorol. Soc. **137**, 553 (2011).
[42]T. Haszpra and T. Tél, J. Atmos. Sci. **70**, 4030 (2013).
[43]T. Tél and M. Gruiz, *Chaotic Dynamics* (Cambridge University Press, Cambridge, 2006).
[44]A. E. Motter, M. Gruiz, G. Károlyi, and T. Tél, Phys. Rev. Lett. **111**, 194101 (2013).
[45]E. G. Altmann, J. S. E. Portela, and T. Tél, Phys. Rev. Lett. **111**, 144101 (2013).
[46]G. Pianigiani and J. A. Yorke, Trans. Am. Math. Soc. **252**, 351 (1979).
[47]E. G. Altmann, J. S. E. Portela, and T. Tél, Europhys. Lett. **109**, 30003 (2015).
[48]E. G. Altmann, J. S. E. Portela, and T. Tél, Rev. Mod. Phys. **85**, 869 (2013).
[49]G. Froyland, R. M. Stuart, and E. van Sebille, Chaos **24**, 033126 (2014).
[50]H.-L. Zou, M.-L. Li, C. H. Lai, and Y.-C. Lai, Phys. Rev. E **86**, 066214 (2012).
[51]R. Karnatak, G. Ansmann, U. Feudel, and K. Lehnertz, Phys. Rev. E **90**, 022917 (2014).
[52]M. Wolfrum and O. E. Omelchenko, Phys. Rev. E **84**, 015201(R) (2011).
[53]D. P. Rosin, D. Rontani, N. D. Haynes, E. Schöll, and D. J. Gauthier, Phys. Rev. E **90**, 030902(R) (2014).
[54]A. Daitche and T. Tél, New J. Phys. **16**, 073008 (2014).
[55]T. Kreilos, B. Eckhardt, and T. M. Schneider, Phys. Rev. Lett. **112**, 044503 (2014).
[56]X. Ni and Y.-C. Lai, Chaos **21**, 033116 (2011).
[57]T. Kovács, Gy. Bene, and T. Tél, Mon. Not. R. Astron. Soc. **414**, 2275 (2011).
[58]T. Kovács and Zs. Regály, Astrophys. J. Lett. **798**, L9 (2015).
[59]A. B. Schelin, Gy. Károlyi, A. P. S. de Moura, N. Booth, and C. Grebogi, Comput. Biol. Med. **42**, 276 (2012).
[60]G. Závodszky, Gy. Károlyi, and Gy. Paál, J. Theor. Biol. **368**, 95 (2015).
[61]F. Gonzales and C. Jung, J. Phys. A **45**, 265102 (2012).
[62]F. Gonzales, G. Drótos, and C. Jung, J. Phys. A **47**, 045101 (2014).
[63]G. Drótos, F. Gonzales Montoya, C. Jung, and T. Tél, Phys. Rev. E **90**, 022906 (2014).
[64]E. E. Zotos, Nonlinear Dyn. **76**, 1301 (2014).
[65]P. J. Romeiras, C. Grebogi, and E. Ott, Phys. Rev. A **41**, 784 (1990).
[66]T. Bódai, E. G. Altmann, and A. Endler, Phys. Rev. E **87**, 042902 (2013).
[67]M. Ghil, M. D. Chekroun, and E. Simonnet, Physica D **237**, 2111 (2008).
[68]T. Bódai and T. Tél, Chaos **22**, 023110 (2012).
[69]G. Drótos, T. Bódai, and T. Tél, J. Clim. **28**, 3275 (2015).
[70]J. M. Pedrosa, G. G. Carlo, D. A. Wisniacki, and L. Ermann, Phys. Rev. E **79**, 016215 (2009).
[71]S. Nonnenmacher, Nonlinearity **24**, R123 (2011).
[72]M. Novaes, J. Phys. A **46**, 143001 (2013).
[73]R. Yang, L. Huang, Y.-C. Lai, C. Grebogi, and L. M. Pecora, Chaos **23**, 013125 (2013).
[74]G.-L. Wang, L. Ying, Y.-C. Lai, and C. Grebogi, Phys. Rev. E **87**, 052908 (2013).
[75]M. Schonwetter and E. G. Altmann, Phys. Rev. E **91**, 012919 (2015).
[76]H. Cai and J. Wiersig, Rev. Mod. Phys. **87**, 61 (2015).
[77]Such sets of noninvertible systems are called chaotic repellers.
[78]There might be a deviation from (1) for very large times, too, due to, e.g., particles sticking to the obstacle's surface.
[79]For simplicity, chaotic diffusion and precipitation was not taken into account in the simulation shown in Fig. 6; the inclusion of these effects would not change the picture qualitatively.[39]
[80]When map f is open, one can define two escape rates: One for the energy, another one (the usual escape rate) for particles.
[81]For the other partial dimension, one also needs to know the negative Lyapunov exponent $\bar{\lambda}'$, and finds it as $D_1^{(2)} = -D_1^{(1)}\bar{\lambda}/\bar{\lambda}'$. The information dimension $D^{(1)}$ of the saddle and D_{1c} of the c-measure are then $D^{(1)} = D_1^{(1)} + D_1^{(2)}$ and $D_{1c} = 1 + D_1^{(2)}$, respectively.